Usefulness of a three-dimensional stereotaxic ROI template on anatomically standardised ^{99m}Tc-ECD SPET

Ryo Takeuchi[1], Yoshiharu Yonekura[2], Hiroshi Matsuda[3], Junji Konishi[4]

[1] Department of Internal Medicine, Division of Nuclear Medicine, Nishi-Kobe Medical Center, Kohjidai 5-7-1, Nishi-ku, Kobe-City, Hyogo-Pref., 651-2273, Japan
[2] Biomedical Imaging Research Center, Fukui Medical University, Fukui, Japan
[3] Department of Radiology, National Center Hospital for Mental, Nervous and Muscular Disorders, National Center of Neurology and Psychiatry, Tokyo, Japan
[4] Department of Nuclear Medicine and Diagnostic Imaging, Graduate School of Medicine, Kyoto University, Kyoto, Japan

Received 20 June and in revised form 31 October 2001 / Published online: 19 January 2002

Abstract. We have constructed a three-dimensional stereotaxic ROI template (3DSRT) on anatomically standardised cerebral blood flow (CBF) single-photon emission tomography (SPET) images to objectively estimate regional CBF (rCBF). The 3DSRT is composed of 259 regions of interest (ROIs) in 11 segments (1, superior frontal; 2, middle and inferior frontal; 3, primary sensorimotor; 4, parietal; 5, angular; 6, temporal; 7, occipital; 8, pericallosal; 9, lenticular nucleus; 10, thalamus; 11, hippocampus) on each side. We measured the rCBF values of the 518 ROIs and calculated the area-weighted average (segmental CBF; sCBF) of the 22 segments based on the rCBF in each ROI. We compared vascular reserve before and after revascularisation surgery using sCBF on anatomically standardised resting and acetazolamide (Acz)-challenged CBF SPET images, which were obtained using an equal-volume-split dual-injection single-day protocol [resting and vascular reserve (RVR) method] in 13 patients who had not suffered any major stroke but did have significant cerebrovascular stenosis. Prior to the evaluation, we examined the sCBF values of 16 subjects with various cerebrovascular conditions (8, normal; 3, lacunar infarction; 2, chronic infarction; 2, meningioma; 1, aneurysm) using physiological saline instead of Acz (placebo study) in order to confirm the reproducibility of the RVR method. In the placebo study we observed excellent linearity $(y=1.444+0.964x)$ between the 352 pairs of baseline (x) and post-placebo (y) sCBF values in the 16 subjects, irrespective of the segment location. In all of the 13 patients, estimation of sCBF demonstrated impaired vascular reserve pre-operatively and improved vascular reserve postoperatively. We conclude that the 3DSRT, which could be identically set on the anatomically standardised images obtained at baseline and after Acz injection, allowed objective assessment of the pre- and postoperative vascular reserve, which was not easy with conventional ROI settings. While 3DSRT appeared useful for the evaluation of regional vascular reserve as well as rCBF, further study is necessary to clarify its general clinical value.

Keywords: Three-dimensional – ROI – SPM99 – ^{99m}Tc-ECD – Acetazolamide

Eur J Nucl Med (2002) 29:331–341
DOI 10.1007/s00259-001-0715-z

Ryo Takeuchi (✉)
Department of Internal Medicine, Division of Nuclear Medicine, Nishi-Kobe Medical Center, Kohjidai 5-7-1, Nishi-ku, Kobe-City, Hyogo-Pref., 651-2273, Japan
e-mail: ryouta@land.linkclub.or.jp
Tel.: +81-78-9933727, Fax: +81-78-9933728

Introduction

Statistical parametric mapping (SPM) was originally designed to detect significantly activated regions on positron emission tomography (PET) images [1, 2, 3]. Recently, however, many investigators have tried to apply SPM to single-photon emission tomography (SPET) images to analyse regional cerebral blood flow (rCBF) during the performance of miscellaneous tasks [4, 5, 6] or in neurological disorders [7]. We have also tried to apply SPM for the statistical evaluation of CBF SPET images, but we have been unable to construct a well-documented control SPET database, which is essential for this purpose.

In this study, we utilised SPM99 not for statistical analysis but for anatomical standardisation of rCBF SPET images in order to construct a three-dimensional stereotaxic region of interest (ROI) template (3DSRT) on anatomically standardised SPET images. We compared the cerebrovascular reserve before and after revasculari-

sation surgery using 3DSRT in combination with the resting and vascular reserve method (RVR method) [8]. The RVR method is a dual-injection single-day protocol that we developed to measure resting and acetazolamide (Acz)-activated (post-Acz) rCBF using technetium-99m L,L-ethyl cysteinate dimer (^{99m}Tc-ECD).

Materials and methods

Protocol of the RVR method. The acquisition protocol was as described in our previous study [8], with modification. Each SPET acquisition time was shortened to 12 min from 17.5 min. The method is briefly summarised in Fig. 1. Acquired SPET images were reconstructed by filtered back-projection using a Ramp filter followed by post-processing filtration using a Butterworth filter (order 8, cut-off 0.62 cycles/cm). Attenuation correction was performed using Chang's method (attenuation coefficient: μ=0.09 cm^2/g). To obtain post-Acz projection data, the first projection data were subtracted from the second SPET data multiplied by 1.041, which was the correction coefficient for the decay of ^{99m}Tc between the first and second SPET studies. Finally, the baseline and post-Acz projection data were reformatted to construct transaxial images parallel to the orbitomeatal line. The pixel size and the slice thickness were 4.5 mm square and 4.5 mm, respectively.

To calculate post-Acz mean CBF (mCBF), a transverse slice containing the basal ganglia (slice thickness 9.0 mm) was produced from the summation of axial SPET images as the reference slice. Baseline and post-Acz mean SPET counts were calculated from ROIs which were placed manually over all structures composed of grey matter, white matter and ventricle of the reference slice. Post-Acz mCBF was calculated from baseline mCBF and the SPET counts of the reference slices using Lassen's linearisation correction algorithm (α=2.59) [9].

Baseline and post-Acz ^{99m}Tc-ECD transaxial SPET images were converted to baseline and post-Acz quantitative rCBF images using baseline mCBF and post-Acz mCBF, respectively, by applying Lassen's linearisation correction algorithm (α=2.59) [10].

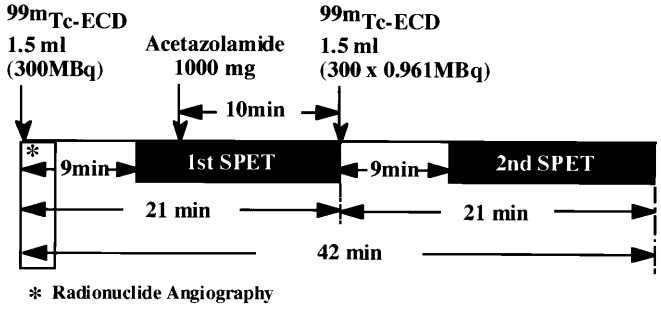

Fig. 1. RVR method. Radionuclide angiography was performed immediately after intravenous bolus injection of 1.5 ml (300 MBq) ^{99m}Tc-ECD, followed by baseline SPET imaging. Acetazolamide was administered during the first SPET acquisition, and immediately after its completion another 1.5 ml (300×0.961 MBq) ^{99m}Tc-ECD was injected. The second SPET acquisition was started 9 min later. The total dose of ^{99m}Tc-ECD was 600 MBq and the total scanning time was 42 min

Anatomical standardisation. To measure rCBF, the quantitative baseline and post-Acz rCBF images were transferred into SPM99, which worked on the MATLAB (MathWorks Inc., Natick, Mass.) Windows software package, and spatially normalised under 12-parameter transformation (Rigid Body, Zooms and Affine) normalisation algorithms – final voxel size, 2 mm×2 mm×2 mm; bounding box, MNI [(–78 mm, –112 mm, –50 mm)–(78 mm, 76 mm, 85 mm)]; interpolation method, bilinear; regularisation, 0.01 (medium); brain mask (Template), apriori/brainmask.img; brain mask (Subject), no use; number of non-linear basis functions, (4, 5, 4); number of iterations of non-linear spatial normalisation, 8 – using qualitative baseline rCBF images as the "Image to determine parameters". Because the distribution of ^{99m}Tc-ECD in the brain is different from that of $H_2{}^{15}O$, which is used as the PET template in the SPM program, for anatomical standardisation we used a ^{99m}Tc-ECD template which Ohnishi et al. made by averaging 14 normal volunteers' ^{99m}Tc-ECD images that were spatially normalised using parameters from co-registered T1-weighted three-dimensional MR images [11].

For a quantitative display of anatomically standardised images, the upper limit of baseline and post-Acz quantitative rCBF images was truncated to 90 before anatomical standardisation. Thereafter, the normalisation processes applied to the truncated images were the same as those applied to the non-truncated images.

Quantitative display of anatomically standardised SPET images. The truncated anatomically standardised 79×95 matrix Analyze format images were transferred to IPLab, a Macintosh-based image processing application (Scanalytics Inc., Fairfax, Va.). Among 68 slices of the transferred image, we used 49 slices (from the 15th to the 63rd), which included transverse slices from the 1_2 (65 mm) to the 10_11 (–24 mm) with slice numbers corresponding to those in the system of Talairach et al. [12]. Adding small pixels with a value of 90 at the corner of each slice of the truncated SPET images to equalise the maximum count of each slice to 90, we applied an identical colour table, which was evenly divided into eight steps from 10 to 90, to each slice in the IPLab.

Construction of 3DSRT on anatomically standardised SPET images. The non-truncated anatomically standardised 79×95 matrix Analyze format images were also transferred to the IPLab and the same 49 slices were processed. Because the abscissa and ordinate in each slice of the IPLab and SPM99 ranged from (0,0) to (94,78) and from (–91,–127) to (89,89), respectively, the converting equations between co-ordinates in SPM99 and the IPLab were: x=2.3Y–91 (1), y=2.3X–127 (2) and z=Z, (3), where (x,y,z) and (X,Y,Z) were the co-ordinates in SPM99 and the IPLab, respectively. Using these equations, we transformed the equations advocated by Brett et al. [13] between co-ordinates in the Talairach atlas [12] and SPM 99 – Xt=0.88x–0.8 (4), Yt=0.97y–3.32 (5), Zt=0.05y+0.88z–0.44 (6), where (Xt,Yt,Zt) were the co-ordinates in the Talairach atlas – into those between the Talairach atlas and the IPLab: X=0.45Yt+53.75 (7), Y=0.49Xt+39.84 (8), Z=1.14Zt–0.056Yt+0.071 (9). We accordingly converted the co-ordinates of the corners of the respective boundaries of anatomical segments on the Talairach atlas into those on the bilateral cortical surfaces of the 49 slices in the IPLab. To decide on the boundaries, we referred to Brodmann's chart of cortical areas and the model of dominant vascularisation reported by Tatu et al. [14]. In total, 518 ROIs were consequently set up, but as this number was considered too large to be evaluated, we grouped them into 11 segments: 1, superior frontal; 2, middle and inferior frontal; 3, primary sensorimotor; 4, parietal; 5, angular; 6, temporal; 7, occipital; 8,

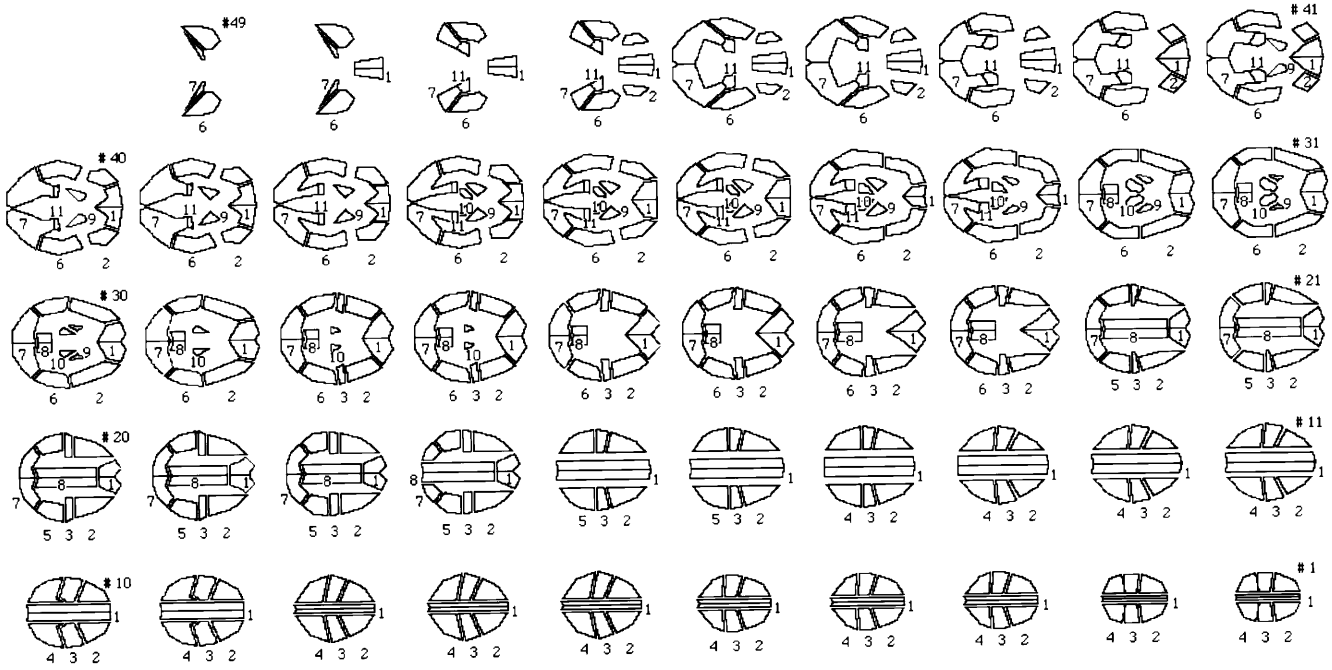

Fig. 2. The 518 ROIs of 3DSRT. *1*, Superior frontal; *2*, middle and inferior frontal; *3*, primary sensorimotor; *4*, parietal; *5*, angular; *6*, temporal; *7*, occipital; *8*, pericallosal; *9*, lenticular nucleus; *10*, thalamus; *11*, hippocampus.

pericallosal; 9, lenticular nucleus; 10, thalamus; 11, hippocampus. These ROIs are illustrated in Fig. 2. We named these 518 ROIs the 3DSRT.

Measurement of rCBF and calculation of sCBF. We measured the rCBF values of the 518 ROIs of 3DSRT automatically with macroprograms using QuicKeys (CE Software, Iowa) software and calculated the area-weighted average for each of the 22 segments based on the rCBF in each of the ROIs. We named this average the segmental CBF (sCBF) value.

Placebo study. To verify the reproducibility of the RVR method in combination with 3DSRT, patients referred to us exclusively for a resting SPET study were examined with the same RVR method using physiological saline instead of Acz. Sixteen subjects (7 women, 9 men; age range 32–80 years) with various cerebral perfusion conditions (8, normal; 3, lacunar infarction; 2, chronic infarction; 2, meningioma; 1, aneurysm) were examined after obtaining their informed consent. We measured sCBF values of the 22 segments before (baseline) and after placebo injection (post-placebo) in each subject, and evaluated the linearity between the two conditions. The 352 pairs of sCBF values of the 16 subjects were analysed. The scatter plot of the baseline sCBF and post-placebo sCBF is illustrated in Fig. 3.

Estimation of pre- and postoperative cerebrovascular reserve. Thirteen patients (2 women, 11 men; age range 51–70 years), who underwent revascularisation surgery (6, superficial temporal artery (STA)–middle cerebral artery (MCA) anastomosis; 4, carotid endarterectomy; 3, carotid stenting) owing to significant stenosis in their internal carotid artery (ICA) or MCA, were followed up. Their clinical symptoms, magnetic resonance imaging (MRI) findings, and magnetic resonance angiography (MRA) findings are summarised in Table 1 together with the mMCBF values, which were the area-weighted average of sCBF of the cortical segments commonly perfused by the MCA (segments 2–6 in Fig. 2). Types of stroke were transient ischaemic attack or reversible ischaemic neurological deficit. None of the strokes were major strokes, but, as already indicated, three lacunar infarctions were included. Ten patients (1 woman, 9 men; age range 51–70 years) had unilateral stenosis localised in the affected hemisphere (unilateral stenosis group). The remaining three patients (1 woman, 2 men; age range 63–70 years) had stenosis bilaterally (bilateral stenosis group), the affected side being determined by MRA findings.

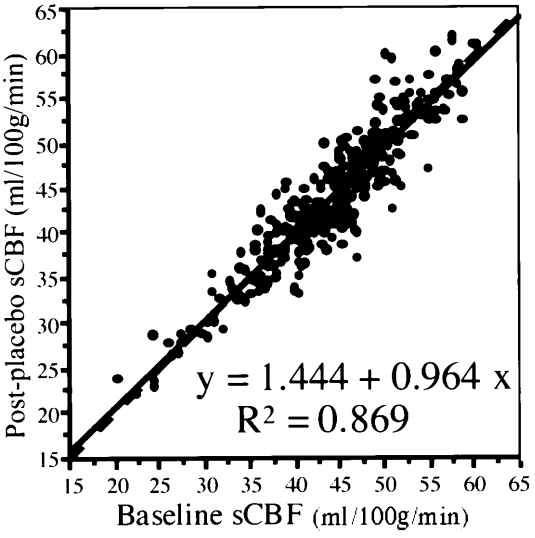

Fig. 3. Scatter plot of baseline sCBFs as measured by post-placebo sCBFs, demonstrating an excellent linearity as determined by linear regression analysis. The *solid line* is the linear regression line, and the *dashed line* is "*y=x*". The regression equation is shown along with the coefficient of determination (R^2)

Table 1. Summary of patients who underwent revascularisation surgery

No./ gender/ age (yr)	Symptom	MRI findings	Vascular lesions	Surgery	Pre operation						Post operation					
					Baseline mMCBF		Post-Acz mMCBF		mMIR		Baseline mMCBF		Post-Acz mMCBF		mMIR	
					Rt	Lt	Rt	Lt	Rt	Lt	Rt	Lt	Rt	Lt	Rt	Lt
1/M/70	Free	Normal	Rt ICA 90% stenosis	Rt S	34.1	34.5	44.9	48.2	1.32	1.40	37.3	37.7	55.3	55.5	1.48	1.47
2/M/51	Muscle weakness of Rt arm	Lacunar	Lt MCA 90% stenosis	Lt A	40.3	38.1	53.9	47.8	1.34	1.25	41.5	36.6	52.2	47.4	1.26	1.29
3/M/66	Muscle weakness of Rt arm	Lacunar	Lt MCA 90% stenosis	Lt A	38.3	34.2	46.5	40.0	1.21	1.17	39.5	36.4	55.2	49.5	1.40	1.36
4/M/69	Lt. amaurosis fugax	Lacunar	Lt ICA 90% stenosis	Lt E	42.9	40.5	51.3	43.4	1.19	1.07	48.9	46.5	61.3	59.8	1.25	1.29
5/M/70	Dysarthria	Normal	Lt ICA 99% stenosis	Lt S	44.1	42.5	64.1	49.7	1.45	1.17	48.6	48.5	76.6	72.8	1.57	1.50
6/M/62	Dysarthria	Lacunar	Rt ICA 99% stenosis	Rt E	38.6	37.9	40.8	40.6	1.06	1.07	41.2	40.8	57.6	56.2	1.40	1.38
7/M/70	Muscle weakness of Rt leg	Lacunar	Lt ICA 99% stenosis	Lt E	39.5	31.6	48.3	37.5	1.22	1.19	42.2	32.7	55.7	45.1	1.32	1.38
8/M/55	Muscle weakness of Rt arm	Lacunar	Lt ICA occlusion	Lt A	34.7	27.0	34.7	29.0	1.00	1.07	34.7	29.0	45.3	33.4	1.31	1.15
9/F/61	Muscle weakness of Rt arm and leg	Lacunar	Lt ICA occlusion	Lt A	41.0	36.5	44.0	36.8	1.07	1.01	47.4	45.7	62.2	52.4	1.31	1.15
10/M/51	Muscle weakness of Rt arm and leg	Lacunar	Lt MCA occlusion	Lt A	48.2	38.7	48.8	34.4	1.01	0.89	44.0	37.0	53.9	45.3	1.23	1.23
11/F/70	Muscle weakness of Lt arm	Lacunar	Rt ICA 99% stenosis Lt ICA 90% stenosis	Rt E	41.2	41.3	38.8	41.8	0.94	1.01	43.6	45.3	57.0	57.1	1.31	1.26
12/M/69	Dizziness (Parkinson's disease)	Lacunar	Lt ICA occlusion Rt ICA 95% stenosis	Lt S	47.4	46.2	47.6	42.0	1.00	0.91	40.2	38.6	52.4	48.4	1.30	1.25
13/M/63	Muscle weakness of Lt arm and leg	Lacunar	Rt ICA occlusion Lt ICA 90% stenosis	Rt A	41.8	41.2	39.5	40.4	0.95	0.98	38.5	36.6	46.0	46.7	1.20	1.27

Lt, Left; Rt, right; MRI, magnetic resonance imaging; ICA, internal carotid artery; MCA, middle cerebral artery; A, STA-MCA anastomosis (STA, superficial temporal artery); E, carotid endarterectomy; S, carotid stenting; mMCBF (unit: ml/100 g/min), the area-weighted average of sCBF of the cortical segments commonly perfused by the MCA (segments 2–6 in Fig. 2); Acz, acetazolamide; mMIR, mean increment ratio of mMCBF (post-Acz mMCBF/baseline mMCBF)

Table 2. Comparison of segmental perfusion before and after operation; unilateral stenosis group

No./gender/ age (yr)	Segment[a]	Pre operation						Post operation					
		Baseline sCBF		Post-Acz sCBF		sIR		Baseline sCBF		Post-Acz sCBF		sIR	
		Rt	Lt	Rt	Lt	Rt	Lt	Rt	Lt	Rt	Lt	Rt	Lt
1/M/70	1	37.6	37.4	48.9	48.5	1.30	1.30	38.4	38.6	55.2	54.6	1.44	1.41
	2	34.5	36.1	44.9	49.7	1.30	1.38	37.9	38.3	55.3	56.6	1.46	1.48
	3	36.8	35.8	44.7	48.5	1.21	1.35	38.1	36.7	56.2	55.5	1.48	1.51
	4	33.7	31.1	45.8	42.5	1.36	1.36	36.4	34.0	55.3	51.2	1.52	1.51
	5	36.0	35.1	53.3	49.4	1.48	1.41	40.3	40.1	55.2	58.8	1.37	1.47
	6	32.0	33.6	43.6	48.5	1.36	1.44	35.8	38.9	55.4	55.5	1.55	1.43
	7	35.5	35.6	50.0	48.6	1.41	1.37	42.1	42.0	64.3	63.2	1.53	1.50
2/M/51	1	42.8	42.1	51.6	59.3	1.21	1.41	42.6	42.2	54.6	51.6	1.28	1.22
	2	39.3	38.9	51.5	51.2	1.31	1.32	41.3	38.9	52.3	48.7	1.27	1.25
	3	37.7	36.0	49.7	41.9	1.32	1.16	39.8	34.0	51.4	45.0	1.29	1.33
	4	40.9	36.4	53.5	43.0	1.31	1.18	40.8	32.1	51.9	41.8	1.27	1.30
	5	42.3	36.7	58.5	40.6	1.38	1.11	42.4	34.5	50.9	50.4	1.20	1.46
	6	42.3	38.8	58.3	48.9	1.38	1.26	42.6	36.8	52.6	48.0	1.24	1.30
	7	43.9	43.5	56.1	59.5	1.28	1.37	44.1	41.1	57.2	53.5	1.30	1.30
3/M/66	1	37.4	35.9	46.3	43.3	1.24	1.21	39.0	38.9	56.2	53.3	1.44	1.37
	2	36.2	33.0	44.1	38.9	1.22	1.18	38.6	35.4	50.5	48.1	1.31	1.36
	3	36.5	32.1	41.7	39.4	1.14	1.23	36.0	33.6	53.7	47.9	1.49	1.43
	4	37.9	32.5	48.1	41.7	1.27	1.28	36.6	33.6	55.3	48.3	1.51	1.44
	5	42.0	39.5	50.1	43.3	1.19	1.10	45.2	41.2	63.5	55.0	1.41	1.33
	6	41.5	36.3	50.8	40.6	1.22	1.12	42.4	39.2	60.9	51.5	1.44	1.31
	7	44.4	42.2	56.7	52.2	1.28	1.24	46.2	44.2	66.3	63.6	1.43	1.44
4/M/69	1	43.2	41.9	50.3	44.3	1.16	1.06	48.6	48.3	64.2	62.1	1.32	1.28
	2	41.1	39.5	48.0	41.6	1.17	1.05	47.4	45.6	57.1	57.0	1.20	1.25
	3	41.2	37.7	49.7	42.7	1.21	1.13	48.7	46.1	61.5	56.9	1.26	1.23
	4	42.0	39.2	52.2	43.3	1.24	1.11	48.0	46.2	64.6	62.4	1.35	1.35
	5	46.0	43.6	50.6	44.0	1.10	1.01	50.7	48.8	62.5	64.1	1.23	1.31
	6	46.1	43.1	56.4	46.1	1.22	1.07	51.2	47.7	65.9	63.4	1.29	1.33
	7	48.9	47.6	58.6	55.4	1.20	1.16	52.9	50.8	69.3	66.2	1.31	1.30
5/M/70	1	45.8	44.8	63.6	56.8	1.39	1.27	52.5	51.7	76.9	78.8	1.47	1.52
	2	44.4	42.9	61.3	50.2	1.38	1.17	49.0	49.9	75.1	74.0	1.53	1.48
	3	47.5	46.6	70.4	51.7	1.48	1.11	49.4	51.0	84.0	77.2	1.70	1.51
	4	46.6	44.6	72.4	50.5	1.55	1.13	54.2	49.5	81.5	74.5	1.50	1.50
	5	46.4	44.3	67.5	49.4	1.45	1.11	54.0	51.7	87.0	78.2	1.61	1.51
	6	40.7	38.8	61.3	47.7	1.51	1.23	44.4	44.2	71.1	67.3	1.60	1.52
	7	43.5	41.9	62.7	59.1	1.44	1.41	47.0	47.2	75.5	72.6	1.61	1.54
6/M/62	1	36.6	36.8	41.0	40.2	1.12	1.09	39.7	39.2	53.7	54.8	1.35	1.40
	2	36.1	35.1	40.3	39.5	1.12	1.12	38.7	38.2	52.6	52.6	1.36	1.37
	3	37.6	37.1	39.3	40.5	1.05	1.09	41.2	40.1	57.0	56.0	1.38	1.40
	4	37.8	38.4	41.2	41.4	1.09	1.08	42.3	44.7	61.1	57.7	1.44	1.29
	5	42.9	45.2	40.1	40.8	0.94	0.90	45.6	47.3	65.7	62.8	1.44	1.33
	6	42.0	40.6	42.3	42.1	1.01	1.04	43.6	42.0	61.9	59.4	1.42	1.41
	7	47.0	45.7	47.1	46.8	1.00	1.02	49.2	48.1	67.5	65.1	1.37	1.35
7/M70	1	42.1	38.5	53.7	47.0	1.27	1.22	42.6	39.3	56.7	52.8	1.33	1.34
	2	39.1	32.2	50.6	39.7	1.29	1.23	40.2	32.1	53.4	43.2	1.33	1.34
	3	41.8	34.2	54.2	43.0	1.30	1.25	44.8	37.2	54.9	52.5	1.23	1.41
	4	37.5	28.6	42.7	30.2	1.14	1.06	39.3	29.7	51.5	39.6	1.31	1.33
	5	40.3	31.0	41.2	31.8	1.02	1.03	45.0	32.5	60.1	47.3	1.34	1.45
	6	39.5	30.6	46.0	35.8	1.16	1.17	44.2	32.6	59.9	45.8	1.35	1.41
	7	43.6	36.0	52.2	43.0	1.20	1.19	51.2	43.0	68.4	57.8	1.34	1.35

Table 2. (continued)

No./gender/ age (yr)	Segment[a]	Pre operation						Post operation					
		Baseline sCBF		Post-Acz sCBF		sIR		Baseline sCBF		Post-Acz sCBF		sIR	
		Rt	Lt	Rt	Lt	Rt	Lt	Rt	Lt	Rt	Lt	Rt	Lt
8/M/55	1	33.6	30.5	32.1	30.7	0.95	1.01	32.1	30.7	42.4	36.7	1.32	1.19
	2	33.0	26.1	32.3	27.2	0.98	1.04	32.3	27.2	42.9	31.5	1.33	1.16
	3	31.2	25.1	34.5	28.1	1.11	1.12	34.5	28.1	41.1	30.7	1.19	1.09
	4	32.6	26.0	31.6	26.9	0.97	1.03	31.6	26.9	43.1	31.4	1.37	1.17
	5	37.3	28.6	36.8	29.7	0.99	1.04	36.8	29.7	51.9	34.2	1.41	1.15
	6	39.1	29.2	38.9	32.7	0.99	1.12	38.9	32.7	50.0	38.1	1.29	1.17
	7	42.2	34.7	42.4	37.9	1.01	1.09	42.4	37.9	54.3	46.0	1.28	1.21
9/F/61	1	40.2	38.9	41.7	38.3	1.04	0.98	47.9	46.1	59.3	58.0	1.24	1.26
	2	39.2	35.1	42.9	34.8	1.09	0.99	46.1	43.6	57.6	49.8	1.25	1.14
	3	38.3	35.7	43.0	35.0	1.12	0.98	45.5	45.3	60.7	50.2	1.33	1.11
	4	41.7	36.5	43.3	41.0	1.04	1.12	48.0	46.2	65.4	54.3	1.36	1.17
	5	45.9	40.4	45.4	39.8	0.99	0.98	52.6	51.7	67.8	57.8	1.29	1.12
	6	43.5	38.2	46.1	38.6	1.06	1.01	48.9	47.3	67.1	55.3	1.37	1.17
	7	46.6	43.4	51.7	43.6	1.11	1.00	54.7	53.2	72.6	66.1	1.33	1.24
10/M/51	1	49.2	46.5	48.9	45.1	0.99	0.97	42.9	42.0	54.2	52.4	1.26	1.25
	2	48.1	40.7	48.9	36.2	1.02	0.89	44.9	39.1	52.7	45.9	1.17	1.18
	3	48.5	40.2	51.3	37.2	1.06	0.93	43.5	36.3	54.9	45.3	1.26	1.25
	4	45.7	36.6	47.9	33.8	1.05	0.93	41.2	34.2	51.2	44.5	1.24	1.30
	5	51.1	37.1	51.2	33.9	1.00	0.91	44.1	36.7	56.7	48.6	1.29	1.32
	6	48.4	36.2	47.2	30.7	0.98	0.85	43.9	35.4	55.5	44.0	1.27	1.24
	7	49.9	47.0	49.4	44.8	0.99	0.95	44.9	41.9	54.9	51.3	1.22	1.22

sCBF, Segmental cerebral blood flow (unit: ml/100 g/min); Acz, acetazolamide; sIR, segmental increment ratio (post-Acz sCBF/baseline sCBF)

[a] 1, 2, 3, 4, 5, 6 and 7 correspond to the segment numbers in Fig. 2, and signify the superior frontal, middle and inferior frontal, primary sensorimotor, parietal, angular, temporal and occipital segments, respectively

To analyse Acz reactivity, the increment ratio (IR) was calculated as post-Acz CBF/baseline CBF. Similarly, mean IR (mIR), mean MIR (mMIR), regional IR (rIR) and segmental IR (sIR) were calculated as post-Acz mCBF/baseline mCBF, post-Acz mMCBF/baseline mMCBF, post-Acz rCBF/baseline rCBF and post-Acz sCBF/baseline sCBF, respectively. We used 1.20 as the threshold IR of the normal Acz response, as reported previously [8].

The sCBF and sIR values under pre-operative baseline and post-Acz conditions were compared with those obtained postoperatively. The results in the unilateral stenosis group (patients 1–10) and the bilateral stenosis group (patients 11–13) are summarised in Tables 2 and 3, respectively.

Example. The patient, a 70-year-old man (patient 1 in Tables 1 and 2), underwent right carotid stenting after being incidentally found to present 90% stenosis of the right ICA. His baseline and post-Acz standardised quantitative SPET images, under pre- and postoperative conditions, are illustrated in Fig. 4. His baseline and post-Acz rCBF in 28 consecutive ROIs of the area perfused by the central artery (segment 3 in Fig. 2), under pre- and postoperative conditions, are summarised in Table 4.

Results

Placebo study

As shown in Fig. 3, there was excellent linearity between the 352 pairs of baseline and post-placebo sCBF values of the 16 subjects irrespective of the segment location. The intercept and the slope of the regression line were 1.444 and 0.964, respectively.

Estimation of pre- and postoperative cerebrovascular reserve

Judging from the mMIR (Table 1), pre-operative impaired Acz reactivity (IR<1.20) was not recognised on either side in the two patients with relatively mild (90%) unilateral stenosis (patients 1 and 2). Postoperatively, impaired vascular reserve was apparent only on the affected side in the two patients with ICA occlusion (patients 8 and 9).

Analysis of sIR values (Tables 2 and 3) showed preoperatively impaired vascular reserve in several seg-

Table 3. Comparison of segmental perfusion before and after operation; bilateral stenosis group

No./gender/ age (yr)	Segment[a]	Pre operation						Post operation					
		Baseline sCBF		Post-Acz sCBF		sIR		Baseline sCBF		Post-Acz sCBF		sIR	
		Rt	Lt	Rt	Lt	Rt	Lt	Rt	Lt	Rt	Lt	Rt	Lt
11/F/70	1	43.5	44.7	41.3	44.7	0.95	1.00	46.1	47.0	59.7	63.6	1.30	1.35
	2	39.5	40.5	35.8	41.2	0.91	1.02	42.1	44.0	50.4	55.4	1.20	1.26
	3	38.1	40.7	38.5	41.2	1.01	1.01	43.0	46.3	58.8	55.8	1.37	1.21
	4	38.4	38.9	38.6	40.9	1.00	1.05	41.8	42.7	54.8	62.0	1.31	1.45
	5	43.7	43.2	41.3	45.4	0.95	1.05	42.9	47.0	64.3	63.6	1.50	1.35
	6	45.8	43.3	42.8	42.7	0.94	0.99	46.7	47.1	64.8	56.9	1.39	1.21
	7	47.2	45.7	47.6	46.4	1.01	1.02	51.0	50.9	67.1	70.1	1.32	1.38
12/M/69	1	47.8	46.7	46.0	43.9	0.96	0.94	51.9	50.4	62.8	60.2	1.21	1.20
	2	45.3	45.8	45.5	40.1	1.01	0.88	48.1	48.1	58.7	54.4	1.22	1.13
	3	52.3	49.4	49.1	44.8	0.94	0.91	58.9	54.8	71.0	59.6	1.21	1.09
	4	49.0	43.6	47.4	39.2	0.97	0.90	57.9	44.3	68.2	53.4	1.18	1.20
	5	52.2	51.8	55.8	45.4	1.07	0.88	55.2	49.6	66.8	58.6	1.21	1.18
	6	46.5	45.1	48.1	43.6	1.04	0.97	47.3	45.2	59.2	55.8	1.25	1.24
	7	49.6	46.6	56.1	53.2	1.13	1.14	53.1	45.5	64.6	59.1	1.22	1.30
13/M/63	1	40.2	41.0	37.5	39.9	0.93	0.97	37.1	37.2	45.5	45.3	1.23	1.22
	2	41.4	41.8	40.0	39.6	0.97	0.95	36.9	35.4	43.7	45.7	1.18	1.29
	3	37.8	39.4	36.7	41.2	0.97	1.05	36.7	36.4	43.5	45.0	1.18	1.24
	4	37.9	40.0	32.9	38.9	0.87	0.97	37.8	36.3	44.9	46.3	1.19	1.28
	5	44.1	43.2	44.5	44.7	1.01	1.03	41.0	39.2	51.2	52.6	1.25	1.34
	6	45.2	41.2	41.5	40.8	0.92	0.99	41.2	38.0	49.8	47.6	1.21	1.25
	7	45.5	43.2	44.4	42.8	0.98	0.99	43.6	43.6	53.7	54.3	1.23	1.24

sCBF, Segmental cerebral blood flow (unit: ml/100 g/min); Acz, acetazolamide; sIR, segmental increment ratio (post-Acz sCBF/ baseline sCBF)

[a] 1, 2, 3, 4, 5, 6 and 7 correspond to the segment numbers in Fig. 2, and signify the superior frontal, middle and inferior frontal, primary sensorimotor, parietal, angular, temporal and occipital segments, respectively

ments in all except one patient (patient 1). Postoperatively, impaired vascular reserve was manifested in 12 segments of three patients (patients 8–10) in the unilateral stenosis group and in six segments of two patients (patients 12 and 13) in the bilateral stenosis group.

In patient 1, the pre-operative sIR value of the primary sensorimotor area (segment 3 in Fig. 2) on the affected side was conspicuous pre-operatively. However, impairment of the vascular reserve in the segment was more precisely estimated on the basis of rCBF and rIR (Table 4). Severe pre-operative impairment of the vascular reserve localised at the segment in the 11th to 16th slices was manifest, while the baseline rCBF values of the affected regions were slightly higher than those on the opposite side. Postoperatively, the vascular reserve was considerably improved bilaterally and baseline rCBFs of the segment were still slightly higher than those on the opposite side. Visual assessment of the quantitative SPET fusion images with 3DSRT (Fig. 4) was also helpful in recognising the regional perfusion conditions.

Discussion

There have been several studies on stereotaxic ROI analysis [15, 16, 17, 18, 19], but in these studies the ROIs themselves were transformed to fit the subjects' individual anatomical arrangements; thus the interindividual anatomical variation remained, and the relation between ROI location and anatomy was not consistent. In contrast to these studies, others have applied a volume of interest (VOI)-based analysis technique (as conventionally used in the study of FDG PET data [20]) to SPET image evaluation [21, 22]. Since the VOI was defined on the anatomically standardised template, automated (semi)-quantification eliminating interobserver variability could be achieved.

In the present study, we also constructed a VOI map, but our aim was the objective estimation of rCBF and cerebrovascular reserve. The arterial territories of the brain have been reported to be hugely variable in size and localisation [23], but standardisation of the location of the arterial territories was essential for automated objective analysis of cerebrovascular conditions. We set up 219 ROIs in superficial grey matter and grouped them into

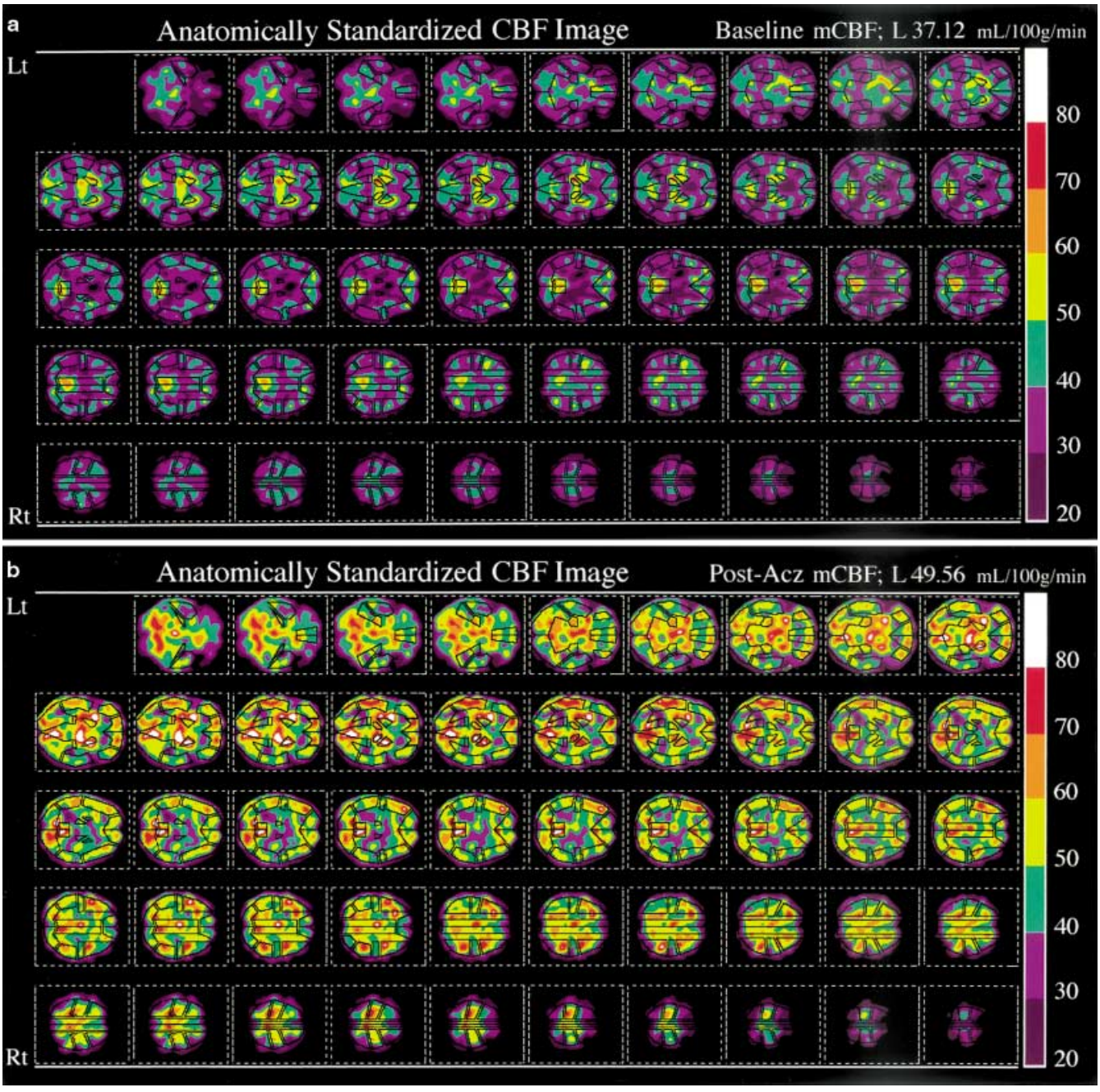

Fig. 4a–d. Anatomically standardised quantitative CBF fusion SPET images with 3DSRT of patient 1 in Tables 1 and 2. **a** Pre-operative baseline image; **b** pre-operative post-Acz image; **c** post-operative baseline image; **d** postoperative post-Acz image. Pre-operative impairment and postoperative improvement in vascular reserve localised from the 11th to the 16th slice in the right primary sensorimotor cortex were observed

eight segments reflecting perfusion areas irrigated by primary branches of cerebral arteries: 1, callosomarginal artery of the anterior cerebral artery (ACA); 2, precentral artery of the MCA; 3, central artery of the MCA; 4, parietal artery of the MCA; 5, angular artery of the MCA; 6, temporal artery of the MCA; 7, posterior cerebral artery; 8, pericallosal artery of the ACA. In addition we set three further groups (40 ROIs: 9, lenticular nucleus; 10, thalamus; 11, hippocampus) and calculated the area-weighted average for each of the 11 segments based on the rCBF in each of the ROIs, to estimate cerebrovascular reserve.

Prior to the analysis of cerebrovascular reserve, we tested 3DSRT in combination with the RVR method using placebo. Excellent reproducibility was confirmed by the linear regression analysis between baseline and placebo-challenged sCBF, as shown in Fig. 3.

We compared the vascular reserve before and after revascularisation surgery in the seven superficially positioned segments using the RVR method with 3DSRT. Although baseline and post-Acz SPET images could be ob-

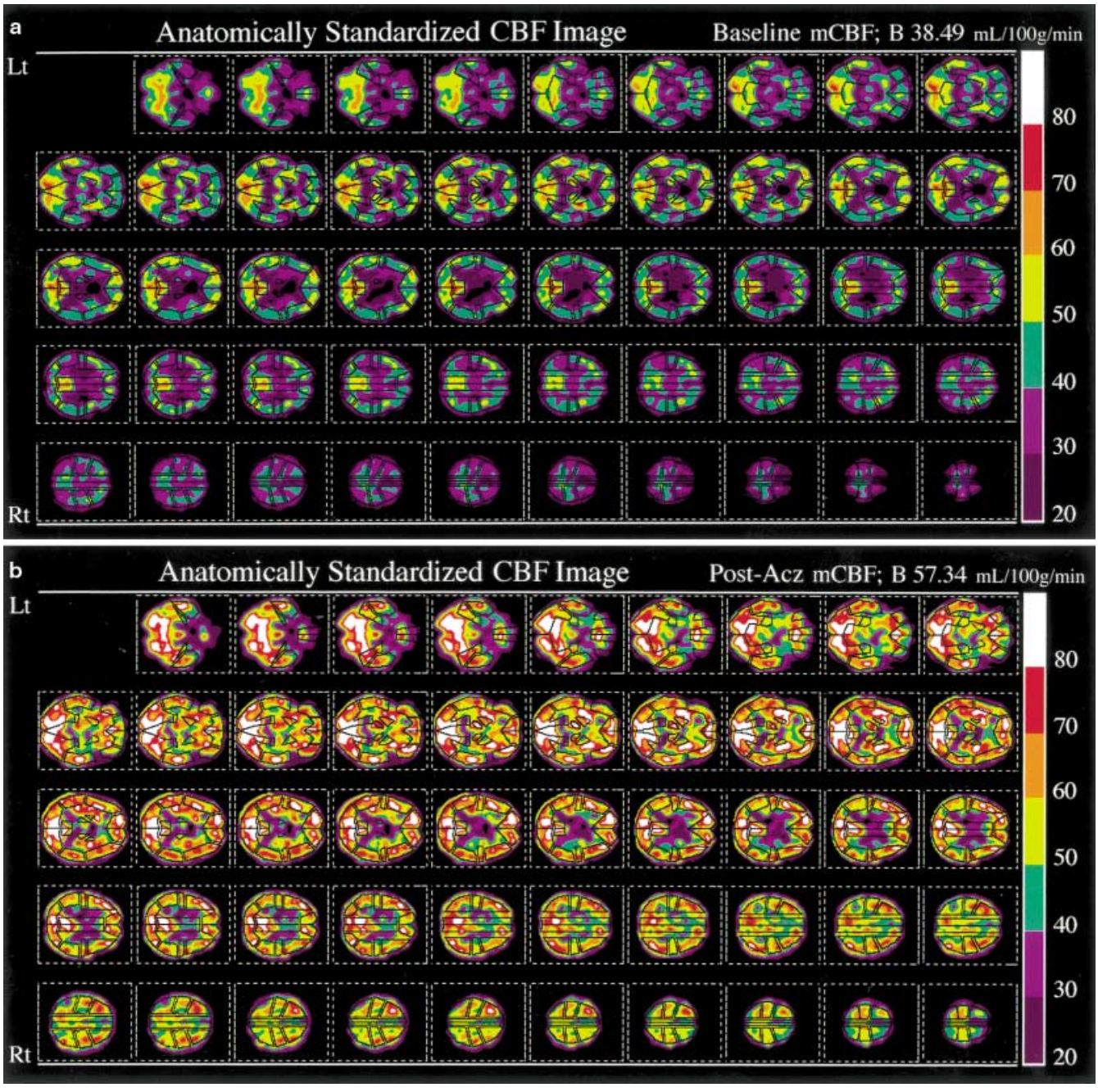

Fig. 4. (continued)

tained without difficulties through the RVR method, estimation of vascular reserve using IR values was not as easy as we had expected because the obtained IR values varied considerably with subtle changes in the shape, size and location of the ROIs. Comparison of the vascular reserve before and after revascularisation surgery was also difficult because it is scarcely possible to achieve identical ROI settings under different conditions using conventional manual ROI delineation, even in the same patient. Since with the RVR method the position of the patient was exactly the same during SPET acquisitions, post-Acz SPET images shared the same anatomical coordinates as baseline ones and could be anatomically standardised using the same movement parameters as were used for baseline images in SPM99. Thus, 3DSRT, which could be identically set on the anatomically standardised images obtained at baseline and after Acz injection, allowed us to objectively assess the pre- and postoperative vascular reserve, which was not possible with conventional ROI settings.

We initially feared that the sCBF evaluation of these segments might be inappropriate for estimation of the vascular reserve because of the vast variation in perfusion pattern. However, in view of the pre- and postopera-

Table 4. Regional CBFs in the primary sensorimotor segment before and after surgery in patient 1

Slice[a]	Rt internal carotid artery 90% stenosis						Post stenting					
	Baseline rCBF		Post-Acz rCBF		rIR		Baseline rCBF		Post-Acz rCBF		rIR	
	Rt	Lt	Rt	Lt	Rt	Lt	Rt	Lt	Rt	Lt	Rt	Lt
1	32.4	33.2	37.1	41.2	1.14	1.24	38.5	35.4	58.5	60.3	1.52	1.70
2	34.6	35.2	40.6	46.2	1.17	1.31	41.1	36.4	59.8	60.3	1.45	1.66
3	34.6	34.8	42.9	47.0	1.24	1.35	38.7	35.1	57.0	56.1	1.48	1.60
4	36.2	36.1	45.9	51.3	1.27	1.42	39.7	36.0	56.8	56.4	1.43	1.57
5	37.7	37.4	48.4	55.3	1.29	1.48	40.4	36.7	57.0	56.6	1.41	1.54
6	37.5	35.7	47.4	51.6	1.26	1.45	37.7	35.9	56.1	54.5	1.49	1.52
7	38.1	36.0	48.1	52.6	1.26	1.46	38.4	36.6	57.6	55.2	1.50	1.51
8	38.4	35.9	48.5	52.7	1.26	1.47	38.7	37.1	58.8	55.7	1.52	1.50
9	37.5	35.6	46.6	48.9	1.24	1.38	38.0	36.7	58.5	55.4	1.54	1.51
10	37.9	36.2	47.5	49.3	1.25	1.36	38.7	37.0	58.6	55.1	1.51	1.49
11	37.0	35.6	41.1	46.4	1.11	1.30	37.6	36.0	57.5	54.3	1.53	1.51
12	37.2	36.3	40.9	47.4	1.10	1.31	38.5	36.6	57.3	54.0	1.49	1.47
13	37.4	36.8	40.2	48.4	1.08	1.32	38.9	37.1	56.5	53.3	1.45	1.44
14	37.9	35.6	38.1	47.1	1.01	1.33	39.5	36.2	54.3	51.8	1.38	1.43
15	37.6	35.4	38.2	47.7	1.02	1.35	39.2	36.3	53.5	51.9	1.36	1.43
16	37.3	35.1	40.2	48.2	1.08	1.37	38.2	36.4	52.5	52.0	1.37	1.43
17	36.3	33.7	42.5	47.1	1.17	1.40	37.4	35.9	51.3	52.4	1.37	1.46
18	35.7	33.7	43.7	47.6	1.22	1.41	36.6	35.9	50.8	53.1	1.39	1.48
19	33.5	34.4	44.8	48.2	1.34	1.40	35.2	36.3	50.2	54.7	1.42	1.50
20	33.5	34.6	44.7	48.0	1.33	1.39	34.8	36.5	50.5	54.9	1.45	1.50
21	34.2	36.6	43.6	45.7	1.28	1.25	36.2	38.5	54.1	58.3	1.50	1.51
22	34.8	37.1	43.2	46.0	1.24	1.24	36.2	39.2	54.6	58.5	1.51	1.49
23	35.4	37.2	43.6	46.6	1.23	1.25	36.6	39.4	55.9	58.5	1.53	1.49
24	36.3	37.4	43.3	47.0	1.19	1.26	36.7	39.8	55.8	58.4	1.52	1.47
25	37.8	36.5	43.2	46.3	1.14	1.27	35.6	37.5	55.4	56.5	1.55	1.51
26	39.1	37.3	44.2	46.4	1.13	1.24	36.1	37.8	55.7	56.4	1.54	1.49
27	41.2	38.0	47.3	47.5	1.15	1.25	37.5	38.3	58.3	56.4	1.55	1.47
28	41.7	39.0	47.5	48.1	1.14	1.23	37.7	38.6	58.1	57.1	1.54	1.48
	Baseline sCBF		Post-Acz sCBF		sIR		Baseline sCBF		Post-Acz sCBF		sIR	
	36.8	35.8	44.7	48.5	1.21	1.35	38.1	36.7	56.2	55.5	1.48	1.51

Abbreviations and acronyms are the same as in Tables 1, 2 and 3

[a] The slice numbers correspond to those in Fig. 2

tive follow-up data shown in Tables 2 and 3, sCBF values may be expected to be useful for the evaluation of cerebrovascular disorders. The vascular reserve in a given area could not be evaluated by reference to the overall mMCBF values of the MCA territory, but could be readily assessed on the basis of the sCBF and sIR. Furthermore, if a more precise evaluation of localised cerebrovascular ischaemia in the early stages were to be required, estimation using rCBF and rIR values simultaneously with sCBF and sIR values could be readily performed, as shown in patient 1 in Table 4. Since vasodilation leading to increased cerebral blood volume is the first response to diminished perfusion pressure as part of an autoregulation mechanism [24], detection of regions with normal resting perfusion but limited vasodilatory potential in a vasodilatory challenge test is essential. The analysis of baseline rCBF values alone was consequently misleading and unsuitable for accurate evaluation of cerebrovascular ischaemia in the early stages.

A voxel-based method like SPM, which compares the differences of two groups with the linear model at each voxel, is effective for the statistical analysis of rCBF changes but unsuitable for evaluation of the CBF in each arterial territory in cerebrovascular disorders. By contrast, VOI-based analysis is suitable for rCBF quantification and especially for quantification of the increase in rCBF in response to Acz challenge. By constructing the 3DSRT we enabled automated quantification of cerebrovascular reserve as well as resting perfusion.

It is concluded that 3DSRT on anatomically standardised rCBF SPET images can be easily used for estimation of cerebral perfusion conditions through numerical as well as visual assessment of rCBF, thereby eliminating interobserver variability.

References

1. Friston KJ, Frith CD, Liddle PF, Frackowiak RSJ. Comparing functional (PET) images: the assessment of significant change. *J Cereb Blood Flow Metab* 1991; 11:690–699.
2. Friston KJ, Frith CD, Liddle PF, Frackowiak RSJ. Plastic transformation of PET images. *J Comput Assist Tomogr* 1991; 15:634–639.
3. Friston KJ, Holmes AP, Worsely KJ, Poline JP, Frith CD, Frackowiak RSJ. Statistical parametric maps in functional imaging: a general linear approach. *Hum Brain Mapping* 1995; 2:189–210.
4. Fukuyama H, Ouchi Y, Matsuzaki S, Nagahama Y, Yamauchi H, Ogawa M, Kimura J, Shibasaki H. Brain functional activity during gait in normal subjects: a SPECT study. *Neurosci Lett* 1997; 228:183–186.
5. Marshall RS, Lazar RM, VanHeertum RL, Esser PD, Perera GM, Mohr JP. Changes in regional cerebral blood flow related to line bisection discrimination and visual attention using HMPAO-SPECT. *Neuroimage* 1997; 6:139–144.
6. Montaldi D, Mayes AR, Barnes A, Pirie H, Hadley DM, Patterson J, Wyper DJ. Associated encoding of pictures activates the medial temporal lobes. *Hum Brain Mapping* 1998; 6:85–104.
7. Ishii K, Yamaji S, Kitagaki H, Imamura T, Hirono N, Mori E. Regional cerebral blood flow difference between dementia with Lewy bodies and AD. *Neurology* 1999; 53:413–416.
8. Takeuchi R, Matsuda H, Yonekura Y, Sakahara H, Konishi J. Noninvasive quantitative measurements of regional cerebral blood flow using technetium-99m-L,L-ECD SPECT activated with acetazolamide: quantification analysis by equal-volume-split ^{99m}Tc-ECD consecutive SPECT method. *J Cereb Blood Flow Metab* 1997; 17:1020–1032.
9. Lassen NA, Andersen AR, Friberg L, Paulson OB The retention of [^{99m}Tc]-*d,l*-HM-PAO in the human brain after intracarotid bolus injection; a kinetic analysis. *J Cereb Blood Flow Metab* 1988; 8 Suppl 1:S13–S22.
10. Matsuda H, Yagishita A, Tsuji S, Hisada K. A quantitative approach to technetium-99m ethyl cysteinate dimer: a comparison with technetium-99m hexamethylpropylene amine oxime. *Eur J Nucl Med* 1995; 22:633–637.
11. Ohnishi T, Matsuda H, Hashimoto T, Kunihiro T, Nishikawa M, Uema T, Sasaki M. Abnormal regional cerebral blood flow in childhood autism. *Brain* 2000; 123:1838–1844.
12. Talairach J, Tournoux P. *Co-planar stereotaxic atlas of the human brain: 3-dimensional proportional system: an approach to cerebral imaging*. Stuttgart: Thieme Medical, 1988.
13. Brett M, Christoff K, Cusack R, Lancaster J. *Using the Talairach atlas with the MNI template.* In: *Human Brain Mapping Conference*. Brighton, UK, 2001.
14. Tatu L, Moulin T, Bogousslavsky J, Duvernoy H. Arterial territories of the human brain; cerebral hemispheres. *Neurology* 1998; 50:1699–1708.
15. Hooper HR, McEwan AJ, Lentle BC, Kotchon TL, Hooper PM. Interactive three-dimensional region of interest analysis of HMPAO SPECT brain studies. *J Nucl Med* 1990; 31:2046–2051.
16. Buck BH, Black SE, Behrmann M, Caldwell C, Bronskill MJ. Spatial- and object-based attentional deficits in Alzheimer's disease: relationship to HMPAO-SPECT measures of parietal perfusion. *Brain* 1997; 120:1229–1244.
17. Jones K, Johnson KA, Becker A, Spiers P, Albert MS, Holman BL. Use of singular value decomposition to characterize age and gender differences in SPECT cerebral perfusion. *J Nucl Med* 1998; 39:965–973.
18. Deutsch G, Mountz JM, Katholi CR, Liu HG, Harrell LE. Regional stability of cerebral blood flow measured by repeated technetium-99m-HMPAO SPECT: implications for the study of state-dependent change. *J Nucl Med* 1997; 38:6–13.
19. San Pedro EC, Deutsch G, Liu HG, Mountz JM. Frontotemporal decreases in rCBF correlate with degree of dysnomia in primary progressive aphasia. *J Nucl Med* 2000; 41:228–233.
20. Liow JS, Rehm K, Strother SC, Anderson JR, Morch N, Hansen LK, Schaper KA, Rottenberg DA. Comparison of voxel- and volume-of-interest-based analyses in FDG PET scans of HIV positive and healthy individuals. *J Nucl Med* 2000; 41:612–621.
21. Van Laere K, Koole M, Versijpt J, Dierckx R. Non-uniform versus uniform attenuation correction in brain perfusion SPET of healthy volunteers. *Eur J Nucl Med* 2001; 28:90–98.
22. Radau PE, Linke R, Slomka PJ, Tatsch K. Optimization of automated quantification of ^{123}I-IBZM uptake in the striatum applied to Parkinsonism. *J Nucl Med* 2000; 41:220–227.
23. Van der Zwan A, Hillen B, Tulleken CAF, Dujovny M. A quantitative investigation of the variability of the major cerebral arterial territories. *Stroke* 1993; 24:1951–1959.
24. Baron JC, Bousser MG, Rey A, Guillard A, Comar D, Castaigne P. Reversal of focal "misery-perfusion syndrome" by extra-intracranial arterial bypass in hemodynamic cerebral ischemia. A case study with ^{15}O positron emission tomography. *Stroke* 1981; 12:454–459.